



Cite this: *Chem. Commun.*, 2024, 60, 10

Structure–activity strategies for mechanically responsive fluorescent materials: a molecular perspective

Guiqiang Fei,^a Shaoqi Li,^a Yuxia Liu,^a Jared B. Carney,^b Tao Chen,^c Yulin Li,^{*c} Xiaoyong Gao,^d Ji Chen,^d Pu Chen,^e Yanfeng Yue,^{ib} Kai Bao,^{*f} Bo Tang^{ib} and Guang Chen^{ib} ^{*,a}

Mechanical response luminescence (MRL) describes the photophysical properties triggered by mechanical stimulation. Usually, MRL can be regulated by intermolecular interactions, molecular conformation or molecular packing, to achieve the desirable optical properties. Herein, at the molecular level, this review covers the factors that influence mechanically responsive fluorescent materials, involving the single- or multifactorial modulation of aliphatic chains, donor–receptor switch, substituent adjustment, and position isomerism. According to these factors, the structure–activity strategies can be summarized as: (i) the self-recovery of optical properties, from the final to initial state, can be regulated by introducing long alkyl chains to a fluorophore. (ii) The sensitivity of MRL materials can be controlled by modifying the donor–acceptor structure via the changed ICT (intramolecular charge transfer) and intramolecular interaction. (iii) The electronic and steric effects of substituents can affect ICT and intermolecular interactions, thereby resulting in high quantum yield and high-contrast MRL materials via changing the molecular stacking of crystalline states. (iv) Intermolecular interaction is modulated by the position isomerism of the substituents, which results in switched molecular packing for the extended response toward a wide range of stimuli. It is anticipated that the molecular mechanisms of these structure–activity relationships will serve as a significant reference for developing novel, high contrast, recyclable mechanical response luminous materials.

Received 11th October 2023,
Accepted 15th November 2023

DOI: 10.1039/d3cc04992b

rsc.li/chemcomm

1. Introduction

Mechanical response luminescence (MRL) is used to describe the results of photophysical characteristic changes, caused by

mechanical stimuli.^{1–3} MRL materials are widely applicable to light-emitting switches, mechanical sensing, security inks, data storage, rewritable paper, anti-counterfeiting and miniature photonic devices, *etc.*^{4–7} Owing to the accessible stimulus of mechanical force, MRL has been widely studied by researchers.⁸ The photophysical properties of solid-state organic molecules are dependent on molecular packing, intermolecular interactions, and molecular conformation. Loose molecular packing, distorted molecular conformations, and weak intermolecular interactions are more likely to respond to external stimuli, which makes it easy to develop novel fluorescent molecules by modulating local structures.^{3,9} To date, there has been fast growth in the number of mechanoresponsive fluorescent compounds developed. However, creating entirely novel light-emitting compounds is both challenging and uncertain. Therefore, current focus is limited to local modification of existing organic fluorophores.¹⁰ The strategy commonly employed for this involves the introduction of long alkyl chains,¹¹ or different substituents to fluorophores, as well as altering donor–receptor interactions^{12–14} or substituent positions. Substituents can adapt the response of solid

^a College of Chemistry and Chemical Engineering Shaanxi University of Science & Technology, Xi'an, 710021, China. E-mail: chenanguang@163.com

^b Department of Chemistry, Delaware State University, Dover, Delaware 19901, USA. E-mail: yyue@desu.edu

^c Northwest Institute of Plateau Biology, CAS, No. 23, Qinghai, 810008, China. E-mail: liyulin@nwipb.cas.cn

^d Jiangsu Simba Biological Medicine Co., Ltd. Gaogang District Qidizhihui Park, Taizhou city, China

^e Department of Chemical Engineering and Waterloo Institute for Nanotechnology, University of Waterloo, 200 University Avenue West, Waterloo, Ontario N2L 3G1, Canada

^f Gordon Center for Medical Imaging, Department of Radiology, Massachusetts General Hospital and Harvard Medical School, Boston, MA, 02129, USA. E-mail: kbao@mgh.harvard.edu

^g College of Chemistry, Chemical Engineering and Materials Science, Key Laboratory of Molecular and Nano Probes, Ministry of Education, Collaborative Innovation Center of Functionalized Probes for Chemical Imaging in Universities of Shandong, Institutes of Biomedical Sciences, Shandong Normal University, Jinan 250014, P. R. China. E-mail: tangb@sdu.edu.cn



Highlight

fluorescent molecules to stimuli and influence the fluorescence quantum yield,^{15–17} whereas introducing long alkyl chains can play an important role in regulating the photoelectric properties of fluorescent molecules.¹⁸ Furthermore, local adjustment of the donor–acceptor structure enables the rapid development of MRL materials.^{13,19–23} Thus, for the further development of high-performance mechanical response luminescence materials, it is necessary to summarize the latest strategies and to discuss the structure–activity relationship from a molecular perspective.

Herein, by studying the factors for mechanical response characteristics, we summarize structure–effect relationships as follows: (i) long alkyl chains occupy a large volume, altering the molecular conformation and generating loose molecular stacking, which results in molecular self-recovery behavior; (ii) the local adjustment of the donor–acceptor structure, such as the substitution of the receptor, the introduction of a spacer, and the use of a donor–acceptor–donor (DAD) molecular structure, alters ICT, intermolecular interaction, and molecular packing. These adjustments increase the sensitivity of the

molecule to external stimuli, and a high-contrast material can be achieved; (iii) substituents can exhibit various spatial effects and electron-withdrawing properties. By screening the substituents, the molecular conformation and molecular packing can be improved, and a high quantum yield, high contrast, and sensitive material can be achieved. (iv) Intermolecular interaction is dependent on the position isomerism of the substituent, leading to changed molecular packing that affects the sensitivity of fluorescent molecules toward external forces (Fig. 1).

At present, most researchers have begun to explore the comprehensive influence of multiple factors on traditional fluorophores. For example, the introduction of halogen atoms and long alkyl chains result in high-contrast multicolor mechanical response, which can be used for color painting (Table 1). Therefore, it is necessary to promptly summarize the recent research on the structure–performance of MRL materials, so as to provide guidance for researchers to further develop MRL materials with high contrast, high response, high emission, and multi-color conversion.



Yulin Li

Yulin Li is a doctoral supervisor at the Northwest Institute of Plateau Biology, Chinese Academy of Sciences, and the Key Laboratory of Tibetan Medicine Research, Chinese Academy of Sciences. He obtained a doctoral degree in science from the Graduate University of Chinese Academy of Sciences in 2007. He is currently the director of the Public Technical Service Center of the Northwest Institute of

Plateau Biology, Chinese Academy of Sciences, and is the leader of natural science and engineering technology disciplines in Qinghai Province.



Yanfeng Yue

Yanfeng Yue is a professor of Chemistry, Delaware State University, Dover, DE, United States. He received his PhD degree in 2008 from Peking University. He focuses on functional molecule design, nanoporous materials and applications in catalysis, and environmental remediation.



Kai Bao

Kai Bao is working on the development of novel contrast agents for the diagnosis and treatment of human diseases. Of particular interest are tumor-targeted NIR fluorophores, where these small molecules can be used for targeting, imaging, diagnosis and therapy by specifically visualizing target tumor cells with high optical properties and minimized nonspecific uptake in normal background tissues.



Bo Tang

Bo Tang is a professor of Chemistry at Shandong Normal University. He received his PhD degree in 1994 from Nankai University. He began his independent career as a professor of chemistry at Shandong Normal University in 1994. He won the National Fund for Outstanding Young Scientists in 2007, and was Chief-scientist for the 973 Program in 2012. He has published more than 300 journal articles, 21 invited book chapters and reviews, and has obtained 39 granted patents.




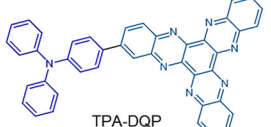
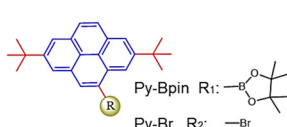
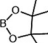

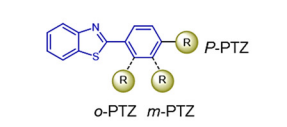
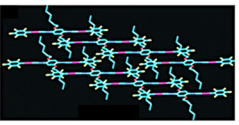
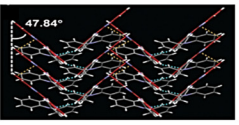
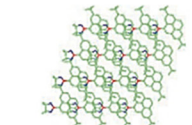
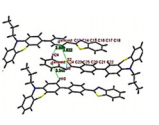
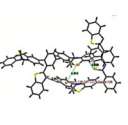
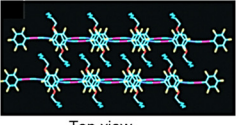
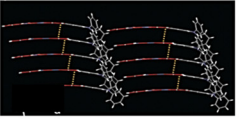
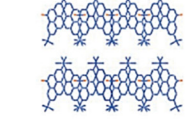
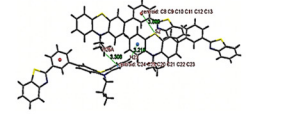
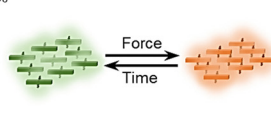
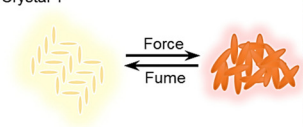
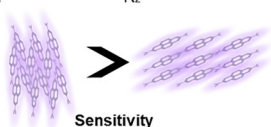
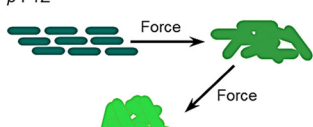
Long chains	Donor-acceptor structure	Different substituents	Position isomerism
 <p>AuIB-Cn</p>	 <p>TPA-DQP</p>	 <p>Py-Bpin R₁:  Py-Br R₂: </p>	 <p>p-PTZ o-PTZ m-PTZ</p>
<p>C₆</p>  <p>Front view</p>	<p>Crystal Y</p>  <p>47.84°</p>	<p>R₁</p> 	<p>p-PTZ</p>  <p>o-PTZ</p> 
 <p>Top view</p>	<p>Crystal-R</p> 	<p>R₂</p> 	<p>m-PTZ</p> 
<p>C₆</p>  <p>Force Time</p>	<p>Crystal Y</p>  <p>Force Fume</p>	<p>R₁ R₂</p>  <p>Sensitivity</p>	<p>p-PTZ</p>  <p>Force</p>
Self-recovery	High-contrast	High-sensitivity	Multi-step response

Fig. 1 Structure–activity relationship of typical compounds.

2. Long chains-effect on MRL performance

2.1 Single-component material fluorescence switching

Recently, some studies have shown that the introduction of long-chain alkyl groups affects the molecular stacking pattern or the molecular conformation, and thereby results in different

photoelectric properties.^{24–26} Therefore, by adjusting the length of peripheral alkyl chains, the optical properties of the initial and grinding states can be regulated. Moreover, the thermal recovery behavior from the grinding state to the initial state can be improved.²⁷ Likewise, the self-recovery rate can also be affected by the length of the alkyl chain.^{11,28} In order to explore the mechanism of long alkyl chains for self-recovery behavior, a series of $[(C_6F_5Au)_2(\mu-1,4\text{-diisocyanobenzene})]$ complexes (AuIB-Cn, $n = 5–10$) were modified with alkyl chains of varying lengths.²⁹ As shown in Fig. 2-(2-1), the general properties of these compounds are a green crystal phase that is converted to an orange amorphous phase after grinding increased fluorescence intensity (Ex = 365 nm). Interestingly, unlike conventional MRL compounds, AuIB-Cn ($n = 5–10$) exhibits unique properties, such as reduced self-recovery time and independence of external stimuli to return to initial state (Fig. 2-(2-1(b))). The principle of this phenomenon lies in that larger alkyl chains increase the spatial tension and thus can rapidly rearrange under the drive of tension, although, the external stimulation disrupts the initial state by increasing the molecular packing disorder and crowded spatial effects (Fig. 2-(2-1(c))). For example, C7 can recover to the initial state quickly at room temperature (20 °C) (<1 s), while C8 recovers much faster than C7, so that this process cannot be captured at 20 °C. (Fig. 2-(2-1(b))). Taking advantage of this, the complexes were used in self-erasable, rewritable paper and flexible, anti-counterfeiting carbon-free carbon paper.



Guang Chen

Guang Chen is a distinguished expert employed by Shaanxi Province, China, and a distinguished professor at the College of Chemistry and Chemical Engineering, Shaanxi University of Science and Technology, Xi'an, China. He received his PhD degree in 2013 from University of Chinese Academy of Science. His research interests include chemical biology, life organic analytical chemistry, functional fluorescent molecular design and bioimaging analysis. He is the leader of the Chemical Imaging Team at Shaanxi University of Science and Technology. He has published more than 100 journal articles, in addition to 20 patents.



Table 1 Summary of all fluorescent molecules

Long chains-effect on MRL performance	
<p> AuIB-Cn $n = 5, 6, 7, 8, 9, 10$ DDCS $\text{R} = \text{C}_{12}\text{H}_{25}$ $\text{CO}_2\text{-R}$ $\text{R} = \text{C}_6\text{H}_{13}$ ($n = 1, 2, 3, 4, 6, 8, 18$) DMQA $\text{R} = \text{CH}_3$ $\text{1b: R} = \text{C}_2\text{H}_5$ $\text{1c: R} = \text{n-C}_3\text{H}_7$ $\text{1d: R} = \text{n-C}_4\text{H}_9$ $\text{1e: R} = \text{n-C}_8\text{H}_{17}$ $\text{1f: R} = \text{n-C}_{10}\text{H}_{21}$ </p>	
Donor-acceptor-effect on MRL performance	
<p> TPA-BPSB, DMAc-BPSB, TPA-DQP, CNDSB (Donor), TCNB (Acceptor), Yam-1, $\text{TPETHC: Linker} = \text{S}$, $\text{TPEHC: Linker} = \text{S}$, $\text{TPEIC: Linker} = \text{no linker}$, Py-BP-PTZ, 1, PTCDI, AQ </p>	
Substituent-effect on MRL performance	
<p> $\text{Ito-1a: R} = \text{H}$, $\text{Ito-1b: R} = \text{Me}$, $\text{Ito-1c: R} = \text{OMe}$, $\text{Ito-1d: R} = \text{OEt}$, $\text{Ito-1e: R} = \text{F}$, $\text{Ito-1f: R} = \text{CF}_3$ $\text{PhMe}_3\text{-BODIPY: R}_1 = \text{R}_2 = \text{R}_3 = \text{CH}_3$ $\text{PhMe-BODIPY: R}_1 = \text{CH}_3, \text{R}_2 = \text{R}_3 = \text{H}$ $\text{Ph-BODIPY: R}_1 = \text{R}_2 = \text{R}_3 = \text{H}$ $\text{IMDMA: R}_1 = \text{H}$, $\text{IMDPA: R}_2 = \text{H}$, $\text{IMCZ: R}_3 = \text{H}$ $\text{Pu-1: R}_1 = \text{R}_2 = \text{H; R}_3 = \text{R}_4 = \text{H}$ $\text{Pu-2: R}_1 = \text{R}_2 = \text{H; R}_3 = \text{R}_4 = \text{H}$ $\text{Pu-3: R}_1 = \text{R}_2 = \text{R}_3 = \text{R}_4 = \text{H}$ $\text{Pu-4: R}_1 = \text{R}_2 = \text{R}_3 = \text{R}_4 = \text{H}$ $\text{Py-Bpin: R}_1 = \text{H}$, $\text{Py-H: R}_2 = \text{H}$ FBKI-thio, $\text{BOPIM-Ph: R} = \text{H}$, $\text{BOPIM-Th: R} = \text{H}$, $\text{BOPIM-TTh: R} = \text{H}$ </p>	
Position isomerism-effect on MRL performance	
<p> $\text{Ito-1: R} = \text{p-Br}$, $\text{Ito-2: R} = \text{m-Br}$, $\text{Ito-3: R} = \text{o-Br}$ Anth-1 (ortho), Anth-2 (meta), Anth-3 (para), Anth-4 (ortho), Anth-5 (meta), Anth-6 (para), p-PTZ, m-PTZ, o-PTZ </p>	
Other effects on MRL performance	Multiple factor-effect on the comprehensive effect of MRL
<p> Cao-1, Cao-1', TBTC </p>	<p> B-1, $\text{Chen-1: R} = \text{C}_6\text{H}_{13}$, $\text{Chen-2: R} = \text{C}_{12}\text{H}_{25}$, c-TAPP, $\text{c-TAPP-T: R} = \text{H}$, $\text{c-TAPP-H: R} = \text{C(CH}_3)_3$ </p>

Multicolor MRL materials have a wide application in both basic science and practical applications.³⁰ In order to explore

the mechanism of long-chain alkyls on polychromatic luminescence, Park *et al.* synthesized the luminescent molecule DDCS



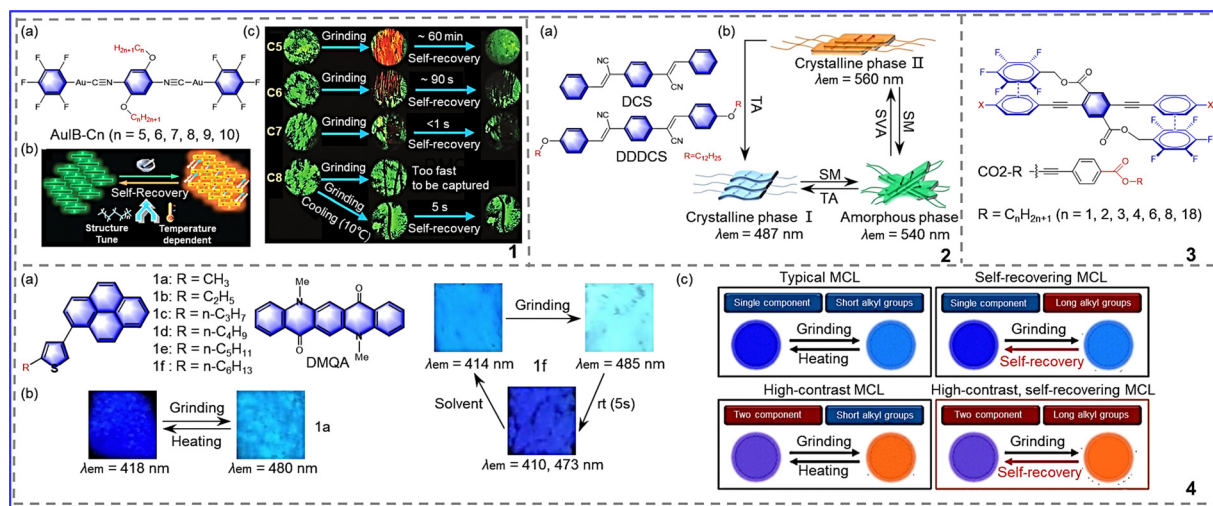


Fig. 2 2-1 (a) Molecular structures of Au(I) complexes AuIB-Cn ($n = 5-10$). (b) Illustration of the proposed mechanochromic luminescence and corresponding self-recovery mechanism of C5-C10. (c) Mechanochromic luminescence and the corresponding self-recoveries of C5-C8 powders. Reprinted with permission from ref. 29. Copyright (2020) Royal Society of Chemistry. 2-2 (a) Chemical structures of the α -DCS derivatives. (b) Three-color cycle of DDDCS. Reprinted with permission from ref. 31. Copyright (2020) Royal Society of Chemistry. 2-3 Chemical structures of compound CO2-R. Reprinted with permission from ref. 32. Copyright (2019) Royal Society of Chemistry. 2-4 (a) Chemical structure of 2-alkyl-4-(pyren-1-yl) thiophenes **1a-f** and *N,N'*-dimethylquinacridone (DMQA). (b) Mechanochromic image of **Ito-1a** and **Ito-1f**. Reprinted with permission from ref. 34. Copyright (2019) Royal Society of Chemistry.

in 2020.³¹ As shown in Fig. 2-(2-2), the α -dicyanodistyryl-benzene (α -DCS) unit serves as the core of DDDCS, flanked by long dodecyloxy chains, providing a reversible high fluorescence, high contrast, and a steady-state multicolor conversion system under different external stimuli. The specific phenomena of mechanical response are as follows. The original DDDCS powder is in an orange crystal state (O state), which can be changed into a blue crystal state (B state, $\lambda_{em} = 487$ nm, $\Phi_F = 0.57$) by thermal annealing, then a green amorphous state (G state, $\lambda_{em} = 540$ nm, $\Phi_F = 0.19$) by grinding, and finally an orange crystal state (O state, $\lambda_{em} = 560$ nm, $\Phi_F = 0.42$) by solvent-vapor exposure (Fig. 2-(2-2(b))). The compound presents an interesting trichromatic transformation because the B and O states are induced by local dipoles in the α -DCS backbone, and the stacking arrangement in the molecular solid is changed by the long dodecyl chain, thus the G state is induced. In addition, the B and O states exhibit higher quantum yields due to the SLE effect in highly crystalline DDDCS. The rate constant analysis shows that the high fluorescence quantum yields of the B and O states can be explained by the different combinations of the K_f and k_{nr} values. (B state: k_f 0.14 ns⁻¹, k_{nr} 0.11 ns⁻¹, O state: k_f = 0.02 ns⁻¹, k_{nr} = 0.03 ns⁻¹). For G state, the rate constant analysis ($K_f = \Phi_F/\tau_F$) and $k_{nr} = ((1 - \Phi_F)/\tau_F)$ presented K_f = 0.03 ns⁻¹ and k_{nr} = 0.12 ns⁻¹, indicating that the G state may consist only of short-range H-dimer/trimer aggregates with antiparallel dipole coupling. Therefore, this G state has the lowest fluorescence quantum yield. In summary, local modification of the fluorophore helped to develop a good mechanical response with a tricolor cycle.

To investigate the mechanism of long alkyl chains on crystal polymorphism, Thomas III *et al.* synthesized a series of seven ester-terminated three-ring phenylene ethynyls,

among which only the lengths of the terminal benzoate alkyl chain are different (Fig. 2-(2-3)).³² Due to the electron-withdrawing properties of ester substituents attached to tricyclic benzene acetylene, the ArF-ArH interaction is weakened. Therefore, simple adjustment of structure can disrupt this equilibrium and thus affect the performance of fluorescent molecules. In this study, the original equilibrium was broken by changing the alkyl chain length, resulting in a mechanical fluorescence response and temperature-sensitive thermal recovery. As a result, these CO2-R compounds showed reversible violet-green mechanical response to grinding. Meanwhile, the temperature of thermal recovery decreased with the increased length of the alkyl chains. For example, the temperatures of thermal recovery for CO2-1 and CO2-2 were 90 °C; while, on account of the reduced kinetic barrier for the transition from a metastable state to a steady state, the temperature required for thermal recovery was only room temperature when the alkyl chain was longer than the propyl group. Thus, introducing long alkyl chains into fluorophores was demonstrated to be an effective way to develop mechanically responsive color-changing materials.

2.2 Multicomponent materials for fluorescence switching

Multicomponent materials can be prepared by mixing different dyes, providing facile availability and a wide switching of emission. Integrated with long alkyl chains, multicomponent materials present excellent self-recovery characteristics.³³ In 2019, Ito *et al.* reported such an adjustment strategy for mechanical response luminescence characteristics (Fig. 2-(2-4)).³⁴ Long alkyl chains were introduced into a regular MRL molecule (2-alkyl-4-(pyren-1-yl) thiophenes), which was then mixed with a dye without MRL properties (*N,N*-dimethylquinacridone). As expected, two interesting properties were observed: (1) a large switch in emission (~ 200 nm) and



Highlight

high contrast from purple (original state) to orange (grinding state), as shown in Fig. 2-(2-4(c)); (2) ability of self-recovery with good repeatability at room temperature from orange (grinding state) to purple (original state). Therefore, rational modification of the multicomponent materials can realize high contrast and self-recovery, which offer promising guidance for the development of novel MRL materials.

3. Donor–acceptor effect on MRL performance

Donor–acceptor replacement of chromophores is the most basic concept and has a solid theoretical basis. Based on the theory of intramolecular charge transfer, the donor–acceptor pair was modified locally to obtain efficient mechanically responsive organic molecules.^{35,36} As is known, triphenylamine is a propeller-shaped photoelectric molecule that is widely used in the development of organic solar dyes, solid-state fluorescence, and mechanical color-changing materials due to its simple structure and easy modification.^{37,38} Given the excellent properties of triphenylamine, Wang *et al.* synthesized cruciform molecules with the same receptor, bis(phenylsulfonyl)benzene (BPSB), but with different donors,³⁹ as shown in Fig. 3-(3-1). **DMAc-BPSB** exhibited regular properties, where after grinding, the emission was redshifted from 521 nm to 546 nm, and the grinding state could be returned to its initial emission after exposure to dichloromethane vapor (Fig. 3-(3-1(b))). Different from **DMAc-BPSB**, **TPA-BPSB** cannot return to the initial emission with dichloromethane vapor but showed a redshift emission of 18 nm compared to the original state (Fig. 3-(3-1(a))). Due to the influences of different donors on molecular aggregation, the

compounds exhibited various final crystalline states: diphenylamine compounds vary from one crystalline state to another crystalline state; while acridine compounds change from a crystalline state to an amorphous state. Li *et al.* synthesized the molecule TPA-DQP, as shown in Fig. 3-(3-2).⁴⁰ The large π conjugated diquinoxaline phenazine (DQP) served as the acceptor due to its large π conjugated skeleton and strong electron-withdrawing capacity, and triphenylamine (TPA) served as the donor due to its excellent electron-donating capacity. Two crystalline form, crystal-Y and crystal-R, were obtained by different means (Fig. 3-(3-2)), which both possess mechanochromic luminescence (MCL) characteristics of transitioning from a crystalline state to an amorphous state. For crystal-Y, due to the relatively weak intermolecular interactions, after grinding, a wide emission wavelength range was exhibited of 576–706 nm, with a color change from a yellow crystalline to a dark-red amorphous state. After being heated in the air to around 240 °C, crystal-Y was transformed into yellow microcrystals, as shown in Fig. 3-(3-2(b)). For crystal R, after grinding, the emission was switched from 698 nm to 706 nm. After exposure to CH_2Cl_2 vapor for 5 min, the emission returned to 694 nm. Moreover, reversible transition between crystal-Y and crystal-R can be achieved *via* heat treatment and by CH_2Cl_2 vapor fuming. This study shows that appropriate donor–receptor pairs play a crucial role in the development of high-contrast MRL materials.

To gain insight into the mechanism of donor–acceptor pairs for luminescent switches, Xu *et al.* reported a series of D–A (donor and acceptor) cocrystals that respond to anisotropic grinding and isotropic compression.⁴¹ As shown in Fig. 4-(4-1(a)), 1,4-bis-*p*-cyanostyrylbenzene (CNDSB) and **TCNB** served, respectively, as the donor (D) and acceptor (A). Due to their simple and rigid molecular structure, **CNDSB** and **TCNB** exhibit

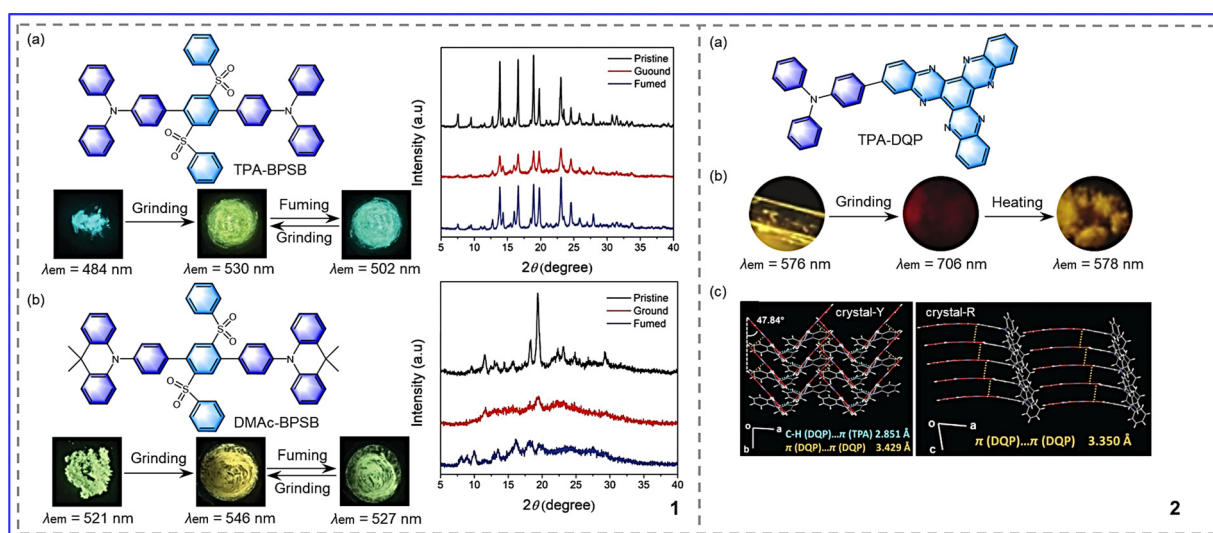


Fig. 3 3-1 (a) Chemical structures of **TPA-BPSB**, photographs of **TPA-BPSB** in response to external stimuli, and PXRD patterns of **TPA-BPSB**. (b) Chemical structures of **DMAc-BPSB**, photographs of **DMAc-BPSB** in response to external stimuli, and PXRD patterns of **DMAc-BPSB**. Reprinted with permission from ref. 39. Copyright (2019) Wiley. 3-2 (a) Molecular structure of TPA-DQP. (b) Fluorescent photographs of crystal-Y in response to external stimuli. (c) PL spectra of crystal-Y in response to external stimuli. Reprinted with permission from ref. 40. Copyright (2020) Wiley.



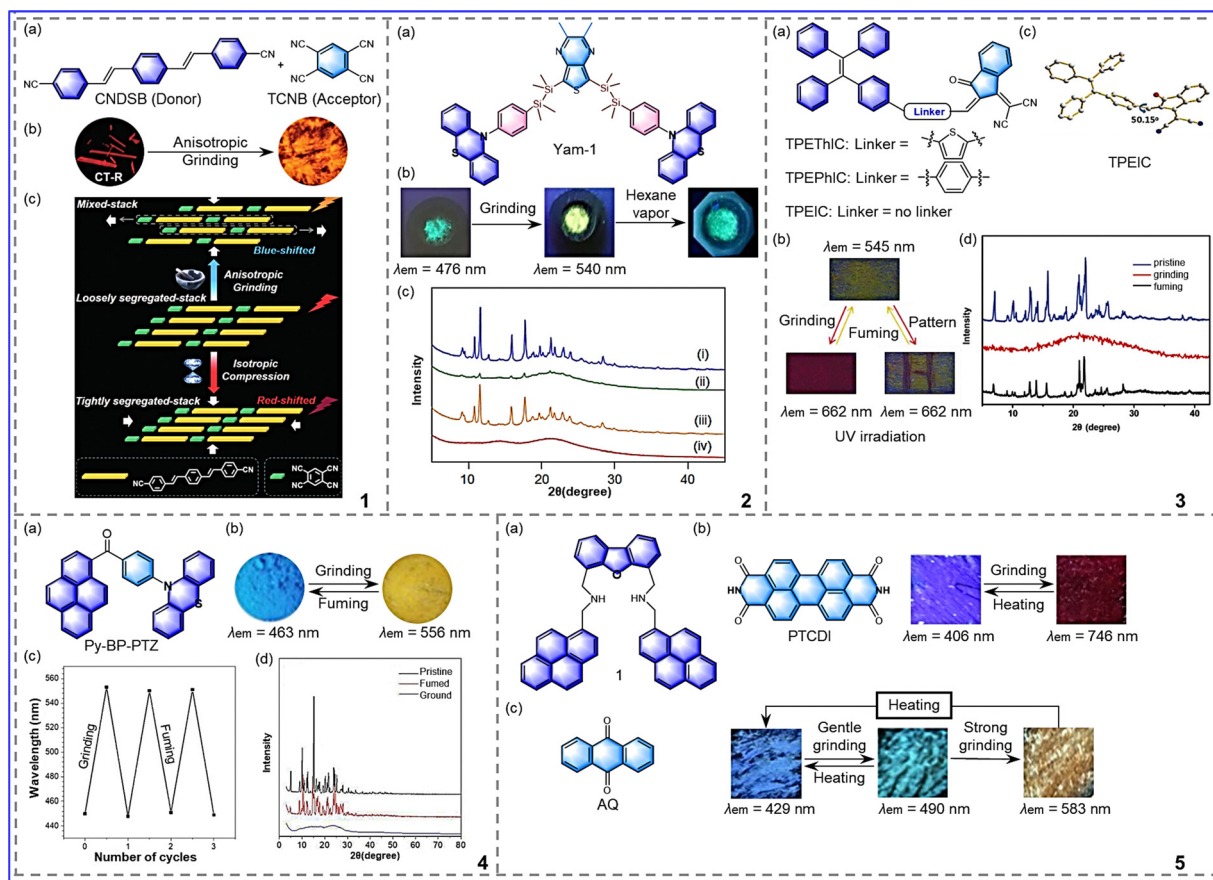


Fig. 4 4-1 (a) Molecular structure of **CNDSD** and **TCNB**. (b) fluorescence images of CT-R cocrystal and (c) mechanism of action of anisotropic grinding and isotropic compression. Reprinted with permission from ref. 41. Copyright (2018) Wiley. 4-2 (a) Chemical structure of **Yam-1**. (b) fluorescence images of **Yam-1** under external stimulus. (c) Powder XRD pattern of **Yam-1**. Reprinted with permission from ref. 42. Copyright (2021) Wiley. 4-3 (a) Chemical structures of **TPETHic**, **TPEPhic** and **TPEIC**. (b) Mechanochromism photographs of TPEIC under 365 nm UV lamp. (c) Single-crystal conformations of TPEIC. (d) X-ray diffraction patterns of TPEIC. Reprinted with permission from ref. 44. Copyright (2019) Royal Society of Chemistry. 4-4 (a) Chemical structure of **Py-BP-PTZ**. (b) Photographs of **Py-BP-PTZ** under UV light during the grinding-fuming process. (c) Reversible cycles of the PL wavelength switching. (d) The PXRD pattern of **Py-BP-PTZ**. Reprinted with permission from ref. 45. Copyright (2020) Royal Society of Chemistry. 4-5 (a) Chemical structure of **1**. (b) Chemical structure of **PTCDI** and photographs of the MCL of 1/PTCDI. (c) Chemical structure of **AQ** and photographs of the MCL of 1/AQ. Reprinted with permission from ref. 46. Copyright (2021) Wiley.

strong crystallization tendency. Thus, a massive CT-R eutectic crystal can be easily obtained upon solvent evaporation. Interestingly, the CT-R eutectic can exhibit different responses to anisotropic and isotropic forces. As shown in Fig. 4-(4-1(b)), with anisotropic force, the sample changed from red to orange, and the fluorescence emission peak showed a unique enhanced hypsochromic shifted emission. The reason for this result lies in that grinding fractured the initial molecular arrangement and rearranged the structure from a segregated stack to a mixed stack, which weakened π - π and CT interactions. In contrast, with an isotropic force, such as hydrostatic pressure, the fluorescence emission peak showed a remarkable bathochromic shifted emission. Because pressure does not disrupt the spatial arrangement, molecules form a closer packing arrangement, which enhances π - π and CT interactions. In conclusion, this study demonstrates that rational molecular design and eutectic engineering strategies not only enable supramolecular control of intermolecular

interactions by forces but also differentiate between the results of isotropic grinding and anisotropic compression forces, allowing one to greatly enrich the chemical properties of MRL materials and broaden their future applications.

In 2021, Yamanoi *et al.* synthesized D-Si-Si-A-Si-Si-D molecules using phenothiazine as a donor and thienopyrazine as an acceptor, as shown in Fig. 4-(4-2).⁴² Because of the flexibility of Si-Si bonds and phenothiazine groups, the molecule has a distorted molecular conformation, resulting in sensitivity to external stimuli. After grinding, the compound **Yam-1** changed from a green crystalline state to a yellow amorphous state, and the maximum emission wavelength redshifted from 476 nm to 540 nm. Then, fumigation with *n*-hexane allowed the initial emission color to be restored, as shown in Fig. 4-(4-2(b), (c)). This showed the potential that the introduction of Si-Si bonds and relatively rigid electron donors can be an effective strategy for developing MRL materials.



Highlight

In recent years, many AIE (aggregation-induced emission) materials with different AIE-active parts have been found to have MRL properties. The introduction of AIE active-parts into molecules can provide effective strategies for the development of MRL materials, with the most common AIE-active part being tetraphenylethylene (TPE).⁴³ Wang *et al.* synthesized three molecules by changing the donor-acceptor spacer group, as shown in Fig. 4-(4-3).⁴⁴ These molecules use TPE as a donor and 1,1-dicyanomethylene-3-indenone (IC) as a receptor. The change in the spacer groups affects the molecular packing and molecular conformation space, resulting in different sensitivity of molecules to grinding. **TPEIC** exhibits the highest mechanical sensitivity among them. **TPEIC** is formed by a single bond connecting a TPE unit and an IC unit, resulting in a more distorted conformation, as shown in Fig. 4-(4-3(c)). After grinding, **TPEIC** changes from the twisted conformation of its crystallized state to the planar conformation of its amorphous state, as shown in Fig. 4-(4-3(d)). The maximum emission is redshifted from 545 nm to 662 nm, and the color changes from yellow to red. The ground **TPEIC** sample was fumigated with CH₂Cl₂ vapor and it returned to its initial state, allowing the cycle to be repeated, as shown in Fig. 4-(4-3(b)). Furthermore, the planar conformations of **TPETHIC** and **TPEPhIC** were converted into a relatively twisted form by grinding, which destroyed the interaction between the hydrogen bond and the stack and shortened the effective conjugate, resulting in a blue-shift in the emission peak. In addition, the three molecules were triggered by ClO⁻ based on the oxidative transformation of the 1,1-dicyanomethylene-3-indanone group into a 1,3-indanedione moiety. Owing to its excellent sensitivity and efficiency, the **TPEIC** probe can sense ClO⁻ in HeLa cells with a distinct yellow fluorescence. As indicated from this study, the direct connection of tetraphene to a functional electron acceptor will provide more sensitive MRL materials.

Tang *et al.* synthesized an asymmetrical D-A-D' molecule (**Py-BP-PTZ**). Benzophenone (BP) was used as an electron acceptor, phenothiazine and pyrene were used as electron donors, as shown in Fig. 4-(4-4).⁴⁵ The molecule has excellent high-contrast properties; its sky blue (463 nm) crystalline state and its yellow (556 nm) amorphous state were observed by repeated grinding and solvent fumigant (DCM), as presented in Fig. 4-(4-4(b)). This property is the result of molecular conformation, intermolecular interaction, and the molecular stacking pattern's comprehensive effect. Due to the high contrast, **Py-BP-PTZ** has a high application value in the fields of information recording and trademark anti-counterfeiting ink. In summary, the D-A-D' structure has great potential value in the development of efficient MRL materials.

In order to achieve reasonable control of the emission wavelength offset under mechanical stimulation, Tachikawa *et al.* prepared organic MCL composites using dibenzofuran-based bis(1-pyrenylmethyl)diamine as a donor and typical organic fluorophores as an acceptor in 2021, as shown in Fig. 4-(4-5).⁴⁶ Due to the segregated crystals' conversion to an amorphous mixture by stimuli based on the FRET (fluorescence resonance energy transfer) mechanism, a wide range of MCL

with emission wavelength shifts of more than 300 nm could be achieved by mixing dibenzofuran-based bis(1-pyrenylmethyl)diamine with 3,4,9,10-perylenetetracarboxylic diimide, as shown in Fig. 4-(4-5). In addition, a two-component mixture of 9,10-anthraquinone can respond to different intensities of mechanical stimulation, as noted by the formation of the excimer of the pyrene reference molecule in 1 upon gentle grinding, followed by the formation of the exciplex between the pyrene group and **AQ** upon strong grinding, as shown in Fig. 4-(4-5). In summary, novel two-component dyes that exhibit a wide range of wavelength shifts or stepwise stimulus-response have the potential to be used in the development of mechanical sensing technologies, which opens up wider possibilities for the development of MRL materials.

4. Substituent effect on MRL performance

In order to develop a tricolor MCL system and explore its mechanism, Ito *et al.* synthesized the phenanthroimidazoly-benzothiadiazoles **Ito-1a-f**, as shown in Fig. 5-(5-1).⁴⁷ These molecules contain different substituents on the phenyl groups of the *para*-position of the benzothiadiazole ring, resulting in a blue shift, red shift, and tricolor MRL, respectively. Due to the relaxation of the twisted conformation by force, **1a** (R = H) can achieve tricolor MRL and red-shift: the emission peak of **1a** is redshifted 20 nm from the green crystalline state ($\lambda_{em} = 526$ nm; $\Phi_F = 0.60$) into the yellow amorphous state ($\lambda_{em} = 546$ nm; $\Phi_F = 0.67$) upon crushing, and then the emission peak is redshifted 19 nm into the orange amorphous state ($\lambda_{em} = 565$ nm; $\Phi_F = 0.54$) upon grinding, followed by a return to the initial state after heating. In addition to **1c**, the other derivatives **1b-1f** also showed a redshift in the emission peak upon grinding and then restoration of the original emission color upon heating. However, the degree of the redshifting in the emission wavelength is affected by the distorted conformation, as shown in Fig. 5-(5-1(b)). For example, the **Ito-1e** molecule exhibits the largest redshifting range due to its high degree of distortion. As for **1c**, an emission peak blueshift was observed upon grinding, resulting from the deformation and distorted restructuring of the molecule conformation. The maximum emission wavelength ($\lambda_{em} = 607$ nm; $\Phi_F = 0.33$) was blue-shifted to 581 nm upon grinding ($\Phi_F = 0.67$). This study shows that the introduction of different substituents can lead to the formation of different crystal structures and achieve different responses to external stimuli.

To develop bright solid-emitting materials, Niu *et al.* synthesized four solid-state luminescent BODIPY derivatives in 2019, as shown in Fig. 5-(5-2).⁴⁸ Due to the introduction of large aromatic groups on the skeleton of BODIPY, the three compounds (PhMe₃-BODIPY, PhMe-BODIPY, and Ph-BODIPY) formed a twisted structure, resulting in loose molecular packing and thus excellent mechanical color-changing properties. Taking PhMe₃-BODIPY as an example, it exhibits unusual high-contrast mechanochromic properties. The red fluorescent



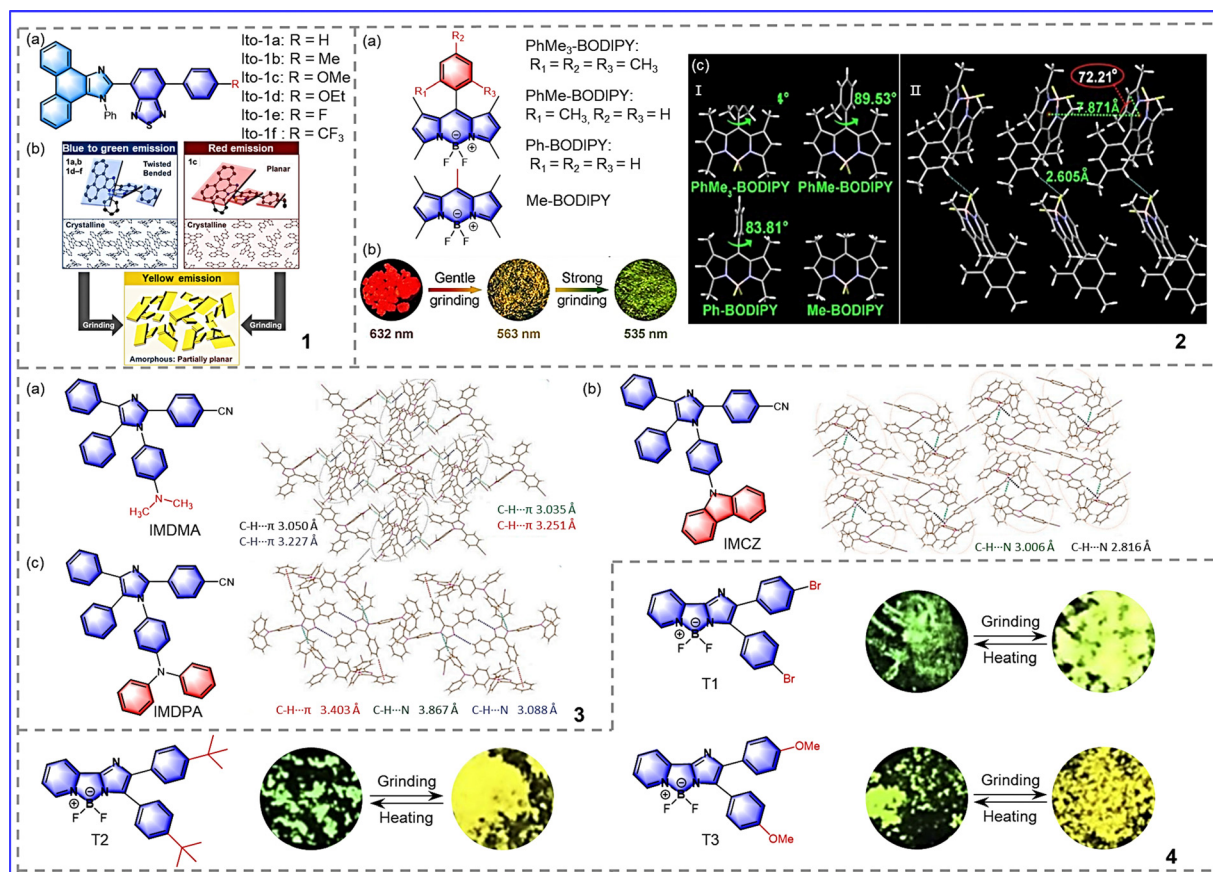


Fig. 5 5-1 (a) Chemical structure of phenanthroimidazoly/benzothiadiazoles **Ito-1a-f**. (b) Schematic representation of the mechanism of **Ito-1a-f**. Reprinted with permission from ref. 47. Copyright (2019) Royal Society of Chemistry. 5-2 (a) Chemical structure of BODIPYs. (b) Photographs of single crystals of PhMe₃-BODIPY after grinding. (c) Single-crystal structures of BODIPYs and molecular packing in the crystal structures of PhMe₃-BODIPY. Reprinted with permission from ref. 48. Copyright (2019) Royal Society of Chemistry. 5-3 Chemical structure and molecular packing of (a) IMDMA, (b) IMCZ, and (c) IMDPA. Reprinted with permission from ref. 49. Copyright (2021) Elsevier. 5-4 (a) Chemical structures of T1, T2 and T3. (b) Photographs of the color changes of T1, T2, and T3 under external stimulus. Reprinted with permission from ref. 50. Copyright (2019) Elsevier.

single crystal ($\lambda_{\text{em}} = 632 \text{ nm}$) turns into a yellow fluorescent microcrystal ($\lambda_{\text{em}} = 563 \text{ nm}$) after gentle grinding and then turns into green amorphous powder ($\lambda_{\text{em}} = 535 \text{ nm}$) after further strong grinding, as shown in Fig. 5-(5-2(b)). The above phenomenon is due to the J-aggregation of single crystals being destroyed by grinding, resulting in microcrystals or powders with a highly distorted conformation, and thus the maximum emission wavelength is blue shifted. More importantly, PhMe₃-BODIPY has the highest fluorescence quantum yield among these compounds (Φ_{F} of up to 32.2%). The steric hindrance of the aryl group at the meso-position of PhMe₃-BODIPY is increased and the energy loss at the excited state is reduced, resulting in an increased fluorescence quantum yield, as shown in Fig. 5-(5-2(c)). Therefore, appropriate substituents can be introduced into the fluorescent molecules so as to achieve control of the solid fluorescence quantum yield, making MRL materials with considerable optical properties.

In order to further explore the structure–packing–property relationship, In 2020, Xia *et al.* synthesized IMCZ, IMDMA, and IMDPA by introducing *N*-carbazolyphenyl, dimethylaminophenyl, and diphenylaminophenyl at the N1 atom of the imidazole core, respectively, as shown in Fig. 5-(5-3).⁴⁹ In the IMCZ crystal,

the rigidity of the CZ group causes the single molecule to occupy a lot of free volume in the crystal, so that the IMCZ molecule can quickly transform from an amorphous form to a crystalline state. Hence, the MRL phenomenon of the IMCZ was not observed. Furthermore, due to the high flexibility of the DMA group, strong intermolecular interactions and π - π dimers form in the crystal state. The strong intermolecular interaction will block the rotation of the dimethyl phenyl group, which leads the maximum emission wavelength to become blue-shifted upon grinding. Unlike the DMA group, the DPA group has moderate flexibility, which makes the IMDPA molecules have appropriate distorted conformation and loose packing in the solid state, and grinding causes the emission wavelength to redshift. The study showed that the selection of flexible substituents leads to different molecular packing and intermolecular interactions, so that MRL materials with different properties can be developed.

To develop novel high-contrast mechanically responsive fluorescent materials, Zhan *et al.* synthesized boron 2-(2'-pyridyl) imidazole (BOPIM) complexes T1, T2 and T3 by introducing different substituents onto the benzene ring of BOPIM dye, as shown in Fig. 5-(5-4).⁵⁰ These compounds have typical intramolecular charge



transfer (ICT) properties. The degree of ICT is the least at T1, followed by T3, and the greatest at T2. It is known that the degrees of ICT can influence photophysical properties under mechanical forces. As expected, the redshift from small to large is T1, T3, and T2. The spectral red shift of T1 was only 22 nm under mechanical stimulation (bright green to yellow-green). In comparison with T1, the maximum emission wavelengths of T2 and T3 were redshifted by 36 nm and 30 nm, respectively. This phenomenon occurs because of the steric effect of the *tert*-butyl group, which results in more loose packing of the crystalline state. This indicates that the electronic and spatial effects of substituents play important roles in the development of mechanically responsive materials with efficient optical properties. In order to develop a new class of MRL molecule with a planar structure and confirm the relationship between molecular packing and mechanochromism, Li *et al.* synthesized pyrene derivatives by introducing different substituents, as shown in Fig. 6-(6-1).⁵¹ Although **Py-H** and **Py-Bpin** have similar mechanical fluorescence responses, they have different sensitivities to stimuli. Upon slight grinding, **Py-Bpin** changed from a purple crystalline (peak at 403 nm, $\Phi_F = 13.44\%$) to bright cyan amorphous material (peak at 466 nm, $\Phi_F = 65.73\%$). However, the original **Py-H** powder needed stronger grinding strength than **Py-Bpin** to induce a color change. The reason for this difference lies in the synergy of the molecular

interactions and molecular packing. Specifically, in **Py-H**, due to the loose stacking of parallel molecules and weak interactions, the applied energy is dissipated through the interlayer slip of the crystal. By contrast, **Py-Bpin** crystals feature the herringbone arrangement paired with strong intermolecular interactions, allowing energy to be used more for molecular packing transitions than for interlayer slip, thus requiring less external force. To sum up, introducing substituents to change intermolecular interactions and molecular stacking makes it possible to develop highly sensitive MRL materials.

Introduction of heteroatoms (N, O, S, *etc.*) to heterocyclic molecules, embedded in the rings, changes the molecular conformation and generates intermolecular and intramolecular hydrogen bonds, such as C–H–N and C–H–O bonds, achieving the modulation of the solid-state optical properties under external stimulation. Therefore, heterocycles are often selected as an effective group in smart luminescent materials.⁵² Because thienyl ring has a spatial effect and a conjugate effect, it can be used for the development of MRL materials. Chujo *et al.* synthesized FBKI-thio molecules by introducing thiophene groups onto the polymorphic luminescent FBKI skeleton, which improved the molecular planarity and promoted the intermolecular electron conjugation, thus enhancing the solid-state molecules' response to external stimuli, as shown

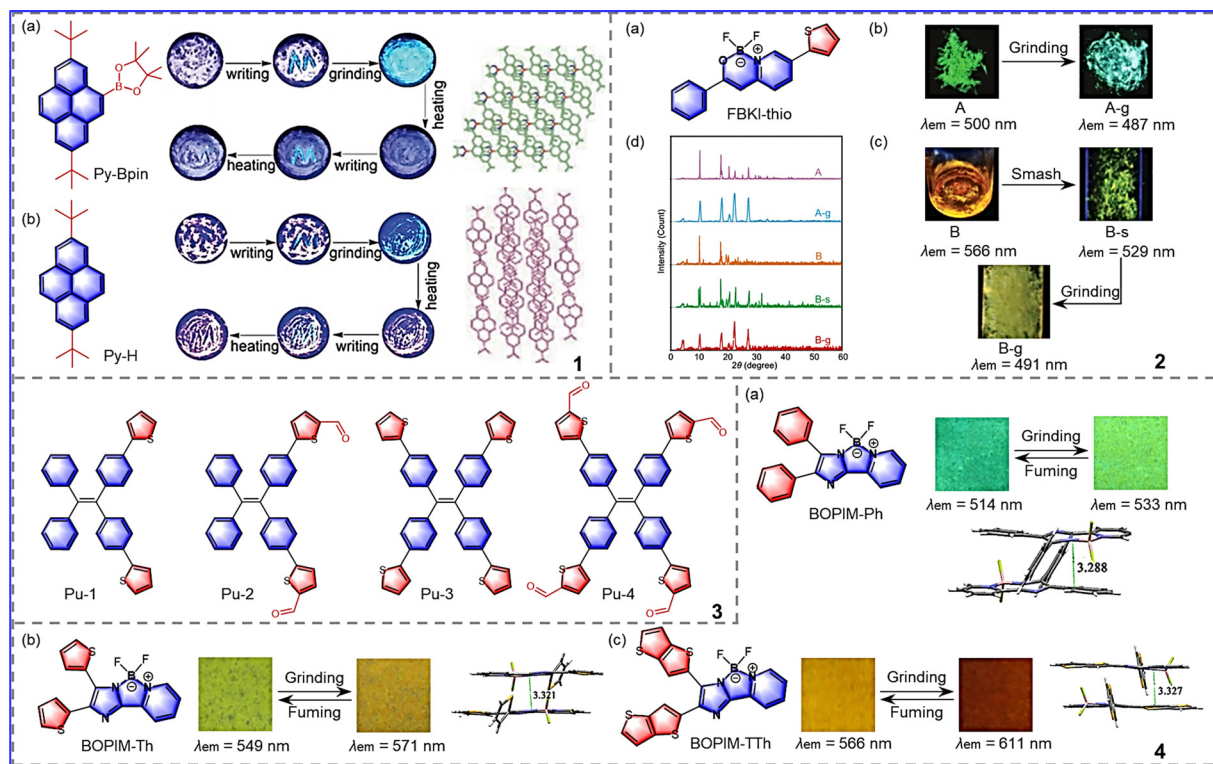


Fig. 6 6-1 Chemical structure, images of mechanochromic experiments and molecular packing of (a) **Py-Bpin** and (b) **Py-H**. Reprinted with permission from ref. 51. Copyright (2018) Wiley. 6-2 (a) Chemical structure of FBKI-thio. Appearances under UV irradiation (365 nm) (b) A and (c) B before and after the mechanical treatments. (d) XRD patterns of FBKI-thio. Reprinted with permission from ref. 53. Copyright (2020) Royal Society of Chemistry. 6-3 The molecular structures of compounds **Pu-1-4**. Reprinted with permission from ref. 54. Copyright (2019) Royal Society of Chemistry. 6-4 The molecular structures, color changes in response to external stimuli, and packing diagrams of (a) **BOPIM-Ph**, (b) **BOPIM-Th** and (c) **BOPIM-TTh**. Reprinted with permission from ref. 55. Copyright (2017) American Chemical Society.



in Fig. 6-(6-2).⁵³ The complex FBKI-Thio can form two types of crystals. Crystal A exhibits common mechanical response properties. The molecular orbital overlap of crystal A decreases by force and the emission peak is blue-shifted as A changes from a green crystalline to a blue amorphous state, as shown in Fig. 6-(6-2(b)). Crystal B exhibits multi-step luminescent chromism, changing from orange to yellow after crushing and then to green after grinding. The PL spectra are blue-shifted, as shown in Fig. 6-(6-2(c)). Because the tightly packed structure is destroyed by crushing, the proportion of disordered structure increases with grinding. In summary, the conjugated properties of the thienyl ring alter the molecular stacking promote the development of sensitive MRL materials.

Pu *et al.* synthesized four thiophene-containing molecules, as shown in Fig. 6-(6-3).⁵⁴ The thiophene and carbonyl units are introduced into the tetraphenylethene, serving to form weak intermolecular interactions. In addition, the tetraphenylethene units form a distorted molecular conformation, leading to loose molecular packing. Therefore, these four molecules are sensitive to the environment. The original solid powder **Pu-1** is transformed from a crystalline state to an amorphous form by grinding, and the initial crystalline form can be restored by fumigation with dichloromethane solvent vapor. The structural transformation of solid samples (**Pu-2**, **Pu-3**, and **Pu-4**) is similar to that of **Pu-1**. Furthermore, the introduction of multiple thiophene groups can increase the red-shift range of the emission wavelength, resulting in different fluorescence colors. In conclusion, this strategy is helpful for the development of panchromatic MRL materials.

Ma *et al.* synthesized 3 BOPIM complexes by introducing different aryl side groups into boron 2-(2'-pyridyl) imidazole

(BOPIM). Due to the introduction of large aromatic donor units, intermolecular interactions and intramolecular charge transfer are enhanced. These complexes show excellent optical properties and mechanochromic responses, as shown in Fig. 6-(6-4).⁵⁵ The bulkier thienothiophene group is one of the most prominent. The group has the most pronounced spatial and electronic effects, so BOPIM-TTh is more sensitive to external forces, producing a wider redshift range (566 nm to 611 nm) and resulting in high-contrast properties. For this reason, bulky aromatic-donating units were introduced into the fluorophore. This modular design strategy can be effectively used to create MRL materials.

5. Position isomerism-effect on MRL performance

A variety of research shows that the introduction of different substituents is an effective way to develop mechanochromic compounds, but its effect may be controlled by position.⁵⁶ In order to explore the effect of substituent position isomerism, Ito *et al.* synthesized a series of phenanthroimidazolylbenzothiadiazole derivatives by changing the bromo group position on the phenyl group relative to the nitrogen atom of the phenanthroimidazole ring, as shown in Fig. 7-(7-1).⁵⁷ Remarkably, the MRL is affected by the position of the bromo group. **Ito-2** (R = *m*-Br) exhibits typical red-shifted two-color mechanochromic luminescence and changes from a blue crystalline ($\lambda_{em} = 503$ nm) to yellow amorphous ($\lambda_{em} = 571$ nm) form upon grinding. **Ito-1** (R = *p*-Br) exhibits unidirectional two-step mechanochromic luminescence (the emission wavelength is

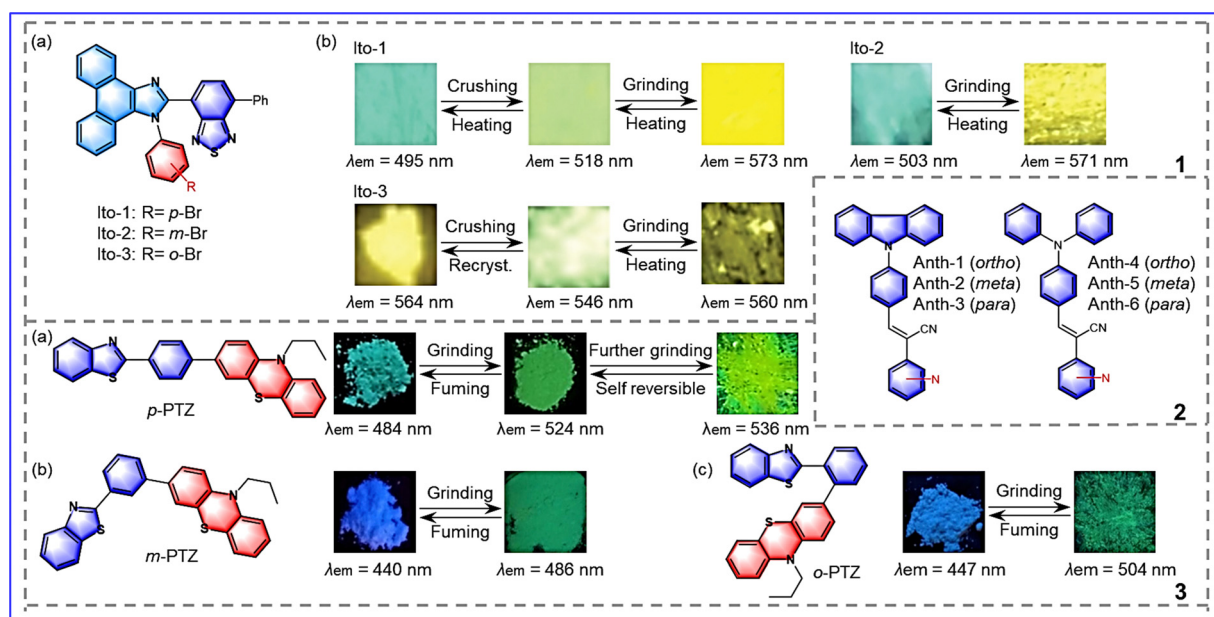


Fig. 7 7-1 (a) The molecular structures of **Ito-1**, **Ito-2**, **Ito-3**. (b) The color changes in response to external stimuli applied to **Ito-1**, **Ito-2**, **Ito-3**. Reprinted with permission from ref. 57. Copyright (2020) Royal Society of Chemistry. 7-2 The molecular structures of **1-6**. Reprinted with permission from ref. 58. Copyright (2021) Royal Society of Chemistry. 7-3 The molecular structures and the color changes in response to external stimuli of (a) *p*-PTZ, (b) *m*-PTZ, (c) *o*-PTZ. Reprinted with permission from ref. 59. Copyright (2020) Royal Society of Chemistry.



gradually redshifted), changing from a blue crystalline ($\lambda_{\text{em}} = 495 \text{ nm}$) to green crystalline ($\lambda_{\text{em}} = 518 \text{ nm}$) form by crushing, and then changing to a yellow amorphous ($\lambda_{\text{em}} = 573 \text{ nm}$) form upon grinding. As for **Ito-3**, it exhibits back-and-forth type mechanochromic luminescence (the emission wavelength is blue-shifted and then red-shifted) and changes from a yellow crystalline ($\lambda_{\text{em}} = 564 \text{ nm}$) into a yellowish green crystalline ($\lambda_{\text{em}} = 546 \text{ nm}$) form by crushing, and then through strong grinding it changes into a yellow amorphous form ($\lambda_{\text{em}} = 560 \text{ nm}$). Thus, changing the position of substituents plays an important role in achieving different emission wavelength shifts.

To explore the effect of the position of nitrogen, Anthony *et al.* synthesized two sets of isomeric molecules, as shown in Fig. 7-(7-2).⁵⁸ The intermolecular interactions in the Anth-1, 2, 3, and 6 lattice are weak and make them sensitive to external stimuli, 4 and 5 do not show any MFC phenomena attributable to molecular packing in the crystal lattice. This study shows that the position of nitrogen influences the formation of fluorescent polymorphs and has a certain effect on the mechanical response performance. Misra *et al.* designed and synthesized *p*-PTZ, *m*-PTZ, and *o*-PTZ (phenothiazine) by changing the position of phenothiazine on the benzene ring, as shown in Fig. 7-(7-3).⁵⁹ *p*-PTZ showed multi-step response to the stimulus. The initial state was green at $\lambda_{\text{em}} = 484 \text{ nm}$, the maximum emission wavelength was redshifted by slight grinding, showing the bright green emission displayed at $\lambda_{\text{em}} = 524 \text{ nm}$. Further grinding resulted in yellow emission at $\lambda_{\text{em}} = 536 \text{ nm}$; the *p*-PTZ could be restored to bright green emission. In addition, *o*-PTZ is the most sensitive to mechanical stimulation due to its weak intermolecular interaction and loose molecular packing. After grinding, it changes from exhibiting blue emission ($\lambda_{\text{em}} = 447 \text{ nm}$) to green emission ($\lambda_{\text{em}} = 504 \text{ nm}$). After fuming with *n*-hexane, the initial state can be restored. Due to the strong intermolecular interaction, *m*-PTZ changes from exhibiting blue emission ($\lambda_{\text{em}} = 440 \text{ nm}$) to green emission ($\lambda_{\text{em}} = 486 \text{ nm}$) after grinding. The results of the research indicate that substituent position isomerism can effectively change the intermolecular interactions and thus affect the solid-state optical properties.

6. Other effects on MRL performance

In addition to the design strategies mentioned above, there are other factors that affect the mechanical response, such as the introduction of boron heteroatoms or controlling the appropriate number of flexible chains.⁶⁰ Cao *et al.* proposed a novel design strategy: introducing BN units into highly planar and large rigid aromatic skeletons, adjusting molecular dipole moments and intermolecular interactions, forming planar quadrilateral molecular stacking, and making molecules more responsive to external stimuli, as shown in Fig. 8-(8-1).⁶¹ The original sample exhibits light-blue emission at 445 nm, and cyan emission is observed at 422 nm and 472 nm after grinding. The mechanical response behavior of **Cao-1** can be attributed to changes in molecular packing and intermolecular

interactions. The position and stacking patterns between adjacent monolayers are changed by grinding, which breaks the sample's crystal structure and transforms it into an amorphous form (Fig. 8-(8-1(c))). Furthermore, the letter JJU is written on the weighing paper (the ink contains the sample dissolved in CH_2Cl_2). After grinding, the letter changes from light blue to cyan, and the initial color can be restored by heating at 100°C for 1 minute, indicating that the sample is optically recording and has potential anti-fake applications. In summary, introducing BN units into conjugated systems to change molecular stacking and intermolecular forces is also a powerful way to develop MRL materials. In addition to introducing boron and nitrogen atoms into the molecule, the introduction of flexible fragments to promote the formation of loose crystal structures is also considered to be a useful strategy to obtain mechanically responsive molecules.⁶² However, a large number of flexible chains will lead to an increase in molecular disorder, which makes it difficult for molecules to crystallize. Therefore, it is very important to control the negative effects of flexible chains on molecules. Huang *et al.* designed and synthesized a stellar-shaped trianiline-benzene-1,3,5-tricarbohydrazide molecule with a twisted molecular conformation, as shown in Fig. 8-(8-2).⁶³ The rigid structure of the central benzene ring and the peripheral rigid triphenylamine (TPA) group can weaken the disorder caused by a large number of flexible chains so that the compound has appropriate crystallization ability. In addition, the TPA unit has a propeller-like conformation and a strong electron-donating ability, which is conducive to the strong solid emission of the compound. Through the above strategies, the negative effects of too many flexible chains can be effectively controlled, and the compound displays mechanical response characteristics. Through recrystallization of the compound, TBTCCH-c and TBTCCH-g single crystals were obtained, respectively, each capable of response to stimuli. The green luminescence of TBTCCH-g turns yellow upon grinding with a reduction in Φ_{F} from 29.2% to 15.5%. The change in fluorescence color is attributed to the transition from a crystalline to an amorphous state. When fumigating the ground samples with ethyl acetate (EA) vapor, the resulting fumigated samples show a blue shift in the emission spectrum of 22 nm and emit yellow-green fluorescence with an increase in Φ_{F} of 27.3%. As for TBTCCH-c, the sample changed from exhibiting blue fluorescence to yellow-green fluorescence with a Φ_{F} value of 28.3% upon grinding. The two crystals can be converted into each other when stimulated. The results show that reasonable design of the molecular structure can overcome the disadvantages of excessive flexible chains and realize the development of polymorphic mechanical discoloration.

7. Multiple factor effect on the comprehensive effect of MRL

In recent years, researchers have not only studied the influence of a single variable on mechanical response performance but have also explored the influence of multiple variables on



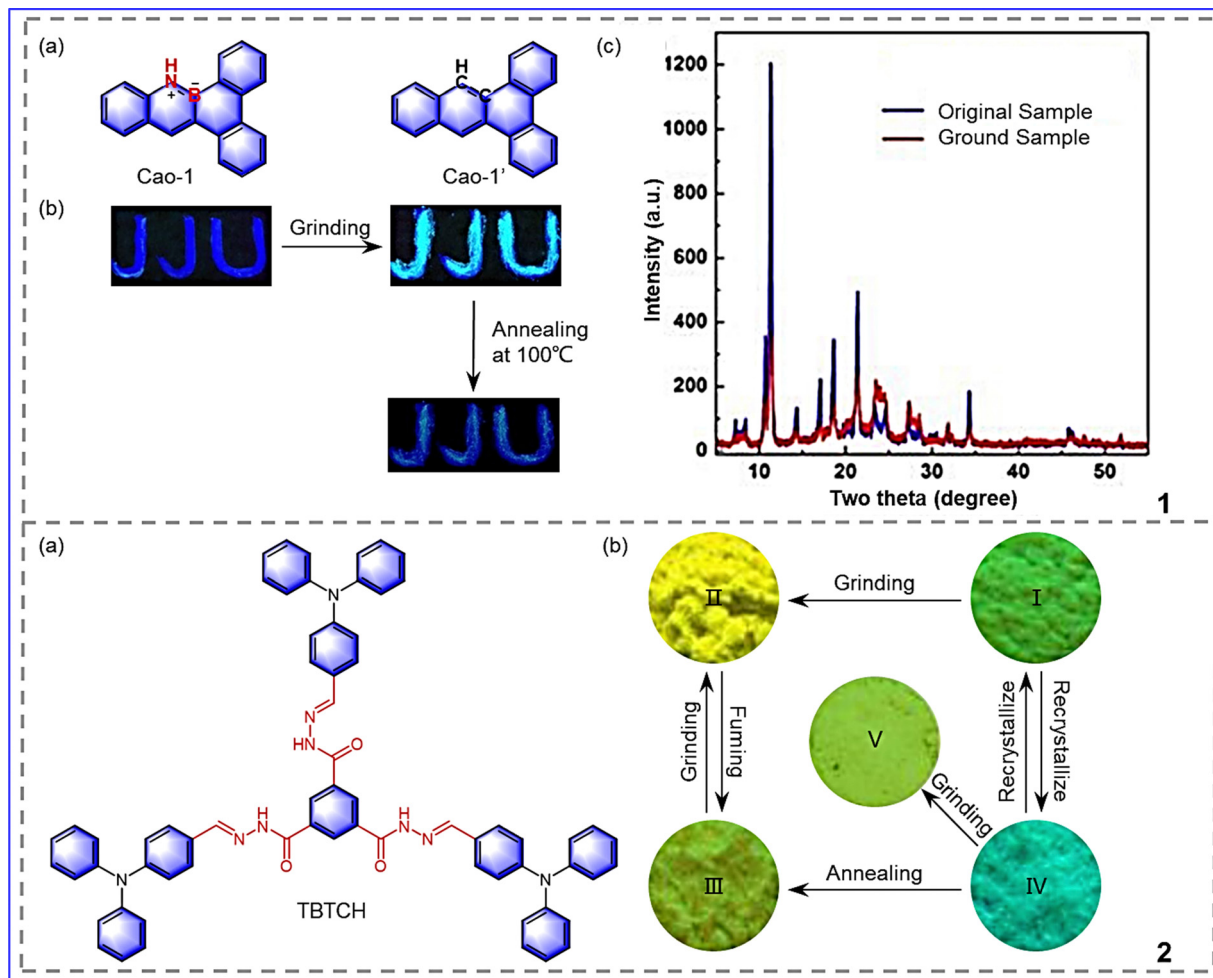


Fig. 8 8-1 (a) The molecular structures of compounds **Cao-1** and **Cao-1'**. (b) Pictures of JJU with different treatments taken under UV irradiation (365 nm). (c) XRD profiles of **Cao-1**; Reprinted with permission from ref. 61. Copyright (2020) Royal Society of Chemistry. 8-2 (a) The molecular structure of TBTCCH (b) Fluorescence images of the solid samples of TBTCCH under 365 nm irradiation: (I) TBTCCH-g; (II) the ground sample of TBTCCH-g; (III) the fumed sample of TBTCCH-g; (iv) TBTCCH-c; (v) the ground sample of TBTCCH-c. Reprinted with permission from ref. 63. Copyright (2020) Royal Society of Chemistry.

traditional fluorophores. Fang *et al.* proposed a simple tetrahedral monoboron complex (**B-1**) with 5,7-diiodine-8-hydroxyquinoline (HQ) as a chelating ligand and hexyl benzene as a single dentate ligand, as shown in Fig. 9-(9-1).⁶⁴ Due to the presence of an iodine substitute (DH8) and an alkyl chain (DB8I), the complex has a tetrahedral geometry and thus forms a distorted molecular conformation. In this way, it lays the foundation for realizing mechanical color-changing responses. In addition, **B-1** is packed in different ways due to the single bond between the two benzene rings and the central boron atom, resulting in the compound being in an amorphous powder (*P*) state and three distinct crystalline states (A, B, and C). These four states are completely interchangeable by grinding and heating. According to this property, many colors (bright green, bright yellow, and bright red) can be obtained by changing the temperature of the solution and paper when using a 2-methyltetrahydrofuran (MTHF) solution of **B-1** as ink, so the complex can be applied in color painting. Therefore, iodine and long alkyl chains are introduced into tetrahedral

complexes, resulting in the development of multicolor MRL materials.

Chen *et al.* developed a new disc-like PAH mesogenic core by introducing S and N heteroatoms, which made the compound form a highly-ordered columnar structure in solution and bulk, as shown in Fig. 9-(9-2).⁶⁵ In addition, introducing the outer alkoxy chain effectively changes the inner column alignment characteristics. The optical properties of the compounds were changed by linking alkoxy chains of different lengths. After grinding, **Chen-1** changes from a yellow-green crystal state to a yellow-brown amorphous state ($\Delta\lambda = 22$ nm), and the absolute fluorescence quantum efficiency Φ_F decreases from 18.7% to 13%. **Chen-2** changes from a green crystalline state to a yellow-brown amorphous state ($\Delta\lambda = 35$ nm), and Φ_F decreases from 14% to 11%. The fuming of the two ground powders with acetone resulted in the emission color of each returning to its initial state, and this mechanical response phenomenon was reproducible. However, **Chen-2** is more sensitive to external stimuli, which may be caused by the long alkyl chain changing



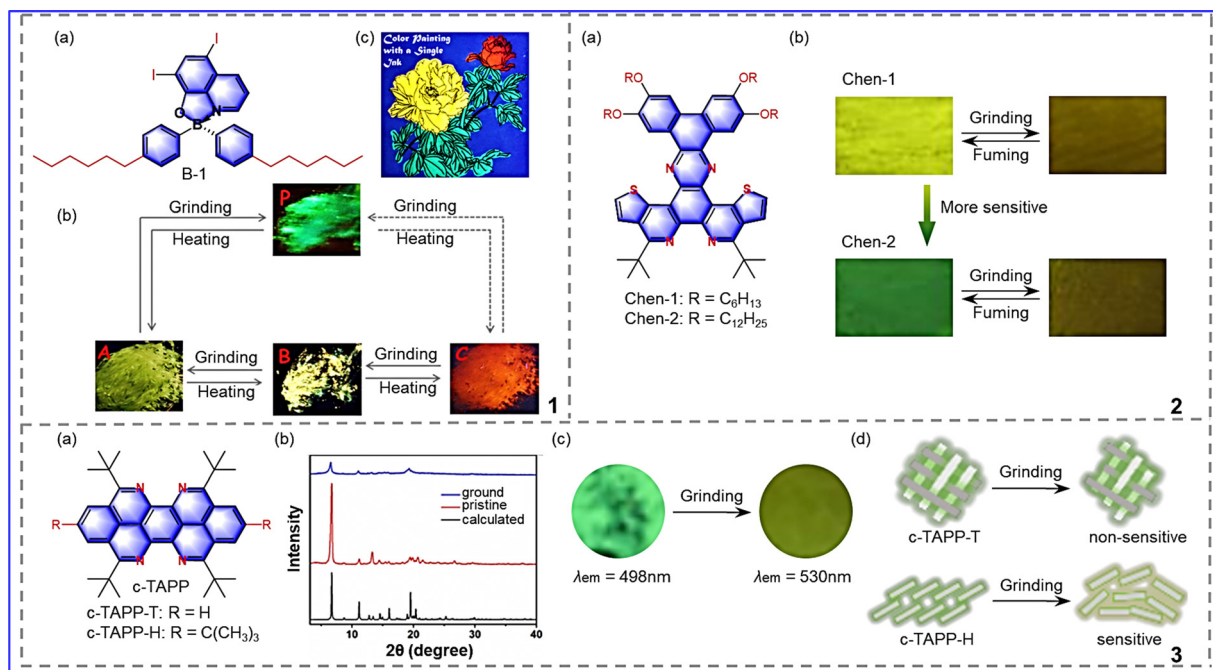


Fig. 9 9-1 (a) Molecular structure of **B-1**. (b) MCL behaviors by polymorphic and (c) Color painting form A–C. Reprinted with permission from ref. 64. Copyright (2019) American Chemical Society. 9-2 (a) Molecular structure of **Chen-1**, **Chen-2**. (b) Photographs in different solid states under 365 nm UV illumination. Reprinted with permission from ref. 65. Copyright (2018) Wiley. 9-3 (a) Chemical structure of **c-TAPP-T** and **c-TAPP-H**. (b) Powder XRD patterns of **c-TAPP-H** under stimulation. (c) Photographs in different solid states under 365 nm UV illumination. (d) Molecular packing changes after grinding. Reprinted with permission from ref. 66. Copyright (2020) Wiley.

the molecular stacking. Therefore, the introduction of heteroatomic sulfur, nitrogen, and long alkyl chains into the original fluorophore can be used for the development of highly-sensitive mechanical response fluorescent materials.

In order to explore the effects of *t*-Bu substitution and regionally selective N-doping on the properties of MCF materials, Chen *et al.* synthesized the first 5, 6, 12, 13-tetrazopyrene derivatives (**c-TAPP-T** and **c-TAPP-H**) by structurally modifying the pyrene core and linking the *t*-Bu side groups, as shown in Fig. 9(9-3).⁶⁶ There is no display of π - π interactions between adjacent azapyrenes in the molecules. This property helps molecules respond to stimuli, but the **c-TAPP-T** have tight cells and multiple intermolecular interactions. Thus, the **c-TAPP-T** crystal is stable and unresponsive to external stimuli. In contrast to **c-TAPP-T**; **c-TAPP-H** possesses loose molecular packing and weak intermolecular interaction. Therefore, the molecule exhibits MRL performance: the green crystalline form changes to a yellow amorphous form after grinding, and the maximum emission wavelength is redshifted by 32 nm. The absolute FL quantum yield changes from 11.8% to 9.7% ($\pm 0.2\%$). The recrystallized samples recover their original emission color after fuming with acetone. That is, the MRL process is repeatable. To sum up, *t*-Bu substitution and regionally selective N-doping can alter the molecular interaction and stacking of molecules. As a result, these strategies are believed to be effective, which is beneficial for obtaining different azapyrene-PAH-based microcrystals and contributes to the development of organic optical devices.

8. Summary and prospectives

In this review, we summarize the recent research on mechanical response luminescence (MRL) materials and structure-activity relationships. The influencing factors for MRL materials involve the effect of long alkyl chains, the effect of different substituents, the change in the donor-acceptor unit, and the effect of position isomerism. We found that (I) the length of the alkyl chain influences the molecular conformation and molecular packing in the solid state, thus affecting the MRL properties. In addition, dyes with MRL properties were mixed with other dyes, and the introduction of long alkyl chains could achieve self-recovery and a high-contrast mechanical response. (II) Changing the donor-acceptor unit (by changing spacer groups, introducing different side chain groups, or adopting eutectic technology) can increase the distortion degree of molecular conformation, improve the molecular crystallization ability, and change the molecular packing, thereby resulting in high quantum yield and high contrast MRL materials. (III) The addition of large aromatic units promotes more twisted conformation and loose molecular packing, thereby improving mechanical stimulation sensitivity. With intramolecular charge transfer properties, groups with ICT, such as halogens and methoxy, display different intermolecular interactions, resulting in a switched maximum emission wavelength in different directions. (iv) Position isomerism affects intermolecular interactions, leading to changed molecular packing for the color switch.



Great progress has been made in MRL materials research in recent years. Many studies have confirmed that local structural modification can produce MRL materials that exhibit excellent performance. Researchers have begun to explore the effect of multiple factors on fluorophore modification, such as halogen atoms and long alkyl chains, which can make the molecules exhibit multi-color mechanical responses. Although rational molecular design and effective control of solid luminescence are particularly challenging, fortunately, the underlying molecular structure–activity relationships are simple and controllable, which contribute to the rapid development of high-contrast, recyclable, and highly-responsive MRL materials.

Conflicts of interest

There are no conflicts to declare.

Acknowledgements

This study was supported by the National Science Foundation of China (22174090); the long-term project of high-level talents innovation in Shaanxi Province (G. C.); the project of National Foreign Senior Expert Program (G2021041002L); and the Natural Science Basic Research Program of Shaanxi (2022JM-089).

Notes and references

- 1 M. Echeverri, C. Ruiz, S. Gamez-Valenzuela, I. Martin, M. C. Ruiz Delgado, E. Gutierrez-Puebla, M. A. Monge, L. M. Aguirre-Diaz and B. Gomez-Lor, *J. Am. Chem. Soc.*, 2020, **142**, 17147–17155.
- 2 Y. Sagara, H. Traeger, J. Li, Y. Okado, S. Schrettl, N. Tamaoki and C. Weder, *J. Am. Chem. Soc.*, 2021, **143**, 5519–5525.
- 3 Y. Sagara, K. Takahashi, A. Seki, T. Muramatsu, T. Nakamura and N. Tamaoki, *J. Mater. Chem. C*, 2021, **9**, 1671–1677.
- 4 X. Zhang, Z. Ma, X. Li, C. Qian, Y. Liu, S. Wang, X. Jia and Z. Ma, *ACS Appl. Mater. Interfaces*, 2021, **13**, 40986–40994.
- 5 G. Huang, Q. Xia, W. Huang, J. Tian, Z. He, B. S. Li and B. Z. Tang, *Angew. Chem., Int. Ed.*, 2019, **58**, 17814–17819.
- 6 P. Alam, N. L. C. Leung, Y. Cheng, H. Zhang, J. Liu, W. Wu, R. T. K. Kwok, J. W. Y. Lam, H. H. Y. Sung, I. D. Williams and B. Z. Tang, *Angew. Chem., Int. Ed.*, 2019, **58**, 4536–4540.
- 7 Z. Wang, F. Yu, W. Chen, J. Wang, J. Liu, C. Yao, J. Zhao, H. Dong, W. Hu and Q. Zhang, *Angew. Chem., Int. Ed.*, 2020, **59**, 17580–17586.
- 8 Y. Yang, X. Fang, S. S. Zhao, F. Bai, Z. Zhao, K. Z. Wang and D. Yan, *Chem. Commun.*, 2020, **56**, 5267–5270.
- 9 S. Fu, X. Feng, N. Zhou, S. Zhang, X. Liu and D. Xu, *J. Lumin.*, 2022, **247**, 118802.
- 10 X. Chang, Z. Zhou, C. Shang, G. Wang, Z. Wang, Y. Qi, Z. Y. Li, H. Wang, L. Cao, X. Li, Y. Fang and P. J. Stang, *J. Am. Chem. Soc.*, 2019, **141**, 1757–1765.
- 11 T. Zhang, Y. Han, K. Wang, M. Liang, W. Bian, Y. Zhang, X. Li, C. Zhang and P. Xue, *Dyes Pigm.*, 2020, **172**, 107835.
- 12 W. Wang, R. Li, S. Xiao, Q. Xing, X. Yan, J. Zhang, X. Zhang, H. Lan and T. Yi, *CCS Chem.*, 2022, **4**, 899–909.
- 13 Y. Chen, X. Zhang, M. Wang, J. Peng, Y. Zhou, X. Huang, W. Gao, M. Liu and H. Wu, *J. Mater. Chem. C*, 2019, **7**, 12580–12587.
- 14 H. Yang, Z. Fu, S. Wang, H. Liu, J. Zhou, K. Wang, X. Wu, B. Yang, B. Zou and W. Zhu, *Mater. Adv.*, 2021, **2**, 4859–4866.
- 15 G. Huang, Y. Jiang, J. Wang, Z. Li, B. S. Li and B. Z. Tang, *J. Mater. Chem. C*, 2019, **7**, 12709–12716.
- 16 Q. Li, H. Zhu and F. Huang, *J. Am. Chem. Soc.*, 2019, **141**, 13290–13294.
- 17 Q. Lai, Q. Liu, K. Zhao, C. Shan, L. Wojtas, Q. Zheng, X. Shi and Z. Song, *Chem. Commun.*, 2019, **55**, 4603–4606.
- 18 Y. Sagara, K. Takahashi, T. Nakamura and N. Tamaoki, *J. Mater. Chem. C*, 2020, **8**, 10039–10046.
- 19 S. Nasiri, A. Dashti, M. Hosseinneshad, M. Rabiei, A. Palevicius, A. Doustmohammadi and G. Janusas, *Chem. Eng. J.*, 2022, **430**, 131877.
- 20 R. Pashazadeh, G. Sych, S. Nasiri, K. Leitonas, A. Lazauskas, D. Volyniuk, P. J. Skabara and J. V. Grazulevicius, *Chem. Eng. J.*, 2020, **401**, 125962.
- 21 S. Liu, Y. Yang, D. D. Deng, X. W. Deng, Z. Chen, X. Y. Wang and S. Pu, *Spectrochim. Acta, Part A*, 2022, **274**, 121122.
- 22 S. Goto, Y. Nitta, N. O. Decarli, L. E. de Sousa, P. Stachelek, N. Tohnai, S. Minakata, P. de Silva, P. Data and Y. Takeda, *J. Mater. Chem. C*, 2021, **9**, 13942–13953.
- 23 S. Wang, L. Li, K. Li, T. Zhang, Z. Zhao and P. Xue, *New J. Chem.*, 2019, **43**, 12957–12962.
- 24 E. L. Heeley, D. J. Hughes, Y. El Aziz, P. G. Taylor and A. R. Bassindale, *Macromolecules*, 2013, **46**, 4944–4954.
- 25 M. Jung, Y. Yoon, J. H. Park, W. Cha, A. Kim, J. Kang, S. Gautam, D. Seo, J. H. Cho, H. Kim, J. Y. Choi, K. H. Chae, K. Kwak, H. J. Son, M. J. Ko, H. Kim, D.-K. Lee, J. Y. Kim, D. H. Choi and B. Kim, *ACS Nano*, 2014, **8**, 5988–6003.
- 26 C. Liu, C. Xiao, J. Wang, B. Liu, Y. Hao, J. Guo, J. Song, Z. Tang, Y. Sun and W. Li, *Macromolecules*, 2022, **55**, 5964–5974.
- 27 H. Wu, Z. Chen, W. Chi, A. K. Bindra, L. Gu, C. Qian, B. Wu, B. Yue, G. Liu and G. Yang, *Angew. Chem., Int. Ed.*, 2019, **58**, 11419–11423.
- 28 S. Ito, S. Nagai, T. Ubukata, T. Ueno and H. Uekusa, *Cryst. Growth Des.*, 2020, **20**, 4443–4453.
- 29 Y. Dong, J. Zhang, A. Li, J. Gong, B. He, S. Xu, J. Yin, S. H. Liu and B. Z. Tang, *J. Mater. Chem. C*, 2020, **8**, 894–899.
- 30 A. Pucci, *Sensors*, 2019, **19**, 4969.
- 31 H.-J. Kim, J. Gierschner and S. Y. Park, *J. Mater. Chem. C*, 2020, **8**, 7417–7421.
- 32 S. A. Sharber, A. Mann, K. C. Shih, W. J. Mullin, M. P. Nieh and S. W. Thomas, 3rd, *J. Mater. Chem. C*, 2019, **7**, 8316–8324.
- 33 S. Ito, G. Katada, T. Taguchi, I. Kawamura, T. Ubukata and M. Asami, *CrystEngComm*, 2019, **21**, 53–59.
- 34 M. Ikeya, G. Katada and S. Ito, *Chem. Commun.*, 2019, **55**, 12296–12299.
- 35 F. Khan, A. Ekbote, S. M. Mobin and R. Misra, *J. Org. Chem.*, 2021, **86**, 1560–1574.
- 36 D. Xu, D. Cheng, Y. Wang, H. Zhou, X. Liu, A. Han and C. Zhang, *Dyes Pigm.*, 2020, **172**, 107786.
- 37 N. Li, H. Liu, Y. Fang, L. Zhang, L. Sui, K. Yuan, G. Wu, K. Wang, B. Yang and B. Zou, *Appl. Phys. Lett.*, 2022, **121**, 111901.
- 38 H. Zhang, J. Zhang, D. Fu, J. Peng, J. Bai and J. Jia, *J. Lumin.*, 2022, **251**, 119199.
- 39 D. Zhou, C. H. Ryoo, D. Liu, S. Wang, G. Qian, Y. Zheng, S. Y. Park, W. Zhu and Y. Wang, *Adv. Opt. Mater.*, 2019, **8**, 1901021.
- 40 H. Yu, X. Song, N. Xie, J. Wang, C. Li and Y. Wang, *Adv. Funct.*, 2020, **31**, 2007511.
- 41 Y. Liu, Q. Zeng, B. Zou, Y. Liu, B. Xu and W. Tian, *Angew. Chem., Int. Ed.*, 2018, **57**, 15670–15674.
- 42 T. Nakae, M. Nishio, T. Usuki, M. Ikeya, C. Nishimoto, S. Ito, H. Nishihara, M. Hattori, S. Hayashi, T. Yamada and Y. Yamanoi, *Angew. Chem., Int. Ed.*, 2021, **60**, 22871–22878.
- 43 H. Wan, S. Zhou, P. Gu, F. Zhou, D. Lyu, Q. Xu, A. Wang, H. Shi, Q. Xu and J. Lu, *Polym. Chem.*, 2020, **11**, 1033–1042.
- 44 H.-X. Yu, J. Zhi, T. Shen, W. Ding, X. Zhang and J.-L. Wang, *J. Mater. Chem. C*, 2019, **7**, 8888–8897.
- 45 Y. Xiong, J. Huang, Y. Liu, B. Xiao, B. Xu, Z. Zhao and B. Z. Tang, *J. Mater. Chem. C*, 2020, **8**, 2460–2466.
- 46 S. Ito, R. Sekine, M. Munakata, M. Yamashita and T. Tachikawa, *Chem. – Eur. J.*, 2021, **27**, 13982–13990.
- 47 S. Nagai, M. Yamashita, T. Tachikawa, T. Ubukata, M. Asami and S. Ito, *J. Mater. Chem. C*, 2019, **7**, 4988–4998.
- 48 C. Duan, Y. Zhou, G.-G. Shan, Y. Chen, W. Zhao, D. Yuan, L. Zeng, X. Huang and G. Niu, *J. Mater. Chem. C*, 2019, **7**, 3471–3478.
- 49 G.-L. Gao, Y.-R. Jia, H. Jiang and M. Xia, *Dyes Pigm.*, 2021, **186**, 109030.
- 50 Y. Zhan, X. Wang, Y. Wang and Y. Xu, *Dyes Pigm.*, 2019, **167**, 1–9.
- 51 Y.-B. Gong, P. Zhang, Y.-R. Gu, J.-Q. Wang, M.-M. Han, C. Chen, X.-J. Zhan, Z.-L. Xie, B. Zou, Q. Peng, Z.-G. Chi and Z. Li, *Adv. Opt. Mater.*, 2018, **6**, 1800198.
- 52 W. Yang, Y. Yang, Y. Qiu, X. Cao, Z. Huang, S. Gong and C. Yang, *Mater. Chem. Front.*, 2020, **4**, 2047–2053.



- 53 S. Saotome, K. Suenaga, K. Tanaka and Y. Chujo, *Mater. Chem. Front.*, 2020, **4**, 1781–1788.
- 54 Y. Yin, Z. Chen, Y. Yang, G. Liu, C. Fan and S. Pu, *RSC Adv.*, 2019, **9**, 24338–24343.
- 55 C. Guo, M. Li, W. Yuan, K. Wang, B. Zou and Y. Chen, *J. Phys. Chem. C*, 2017, **121**, 27009–27017.
- 56 S. Ito, *Chem. Lett.*, 2021, **50**, 649–660.
- 57 S. Takahashi, S. Nagai, M. Asami and S. Ito, *Mater. Adv.*, 2020, **1**, 708–719.
- 58 P. Gayathri, M. Pannipara, A. G. Al-Sehemi, D. Moon and S. P. Anthony, *Mater. Adv.*, 2021, **2**, 996–1005.
- 59 A. Ekbote, S. M. Mobin and R. Misra, *J. Mater. Chem. C*, 2020, **8**, 3589–3602.
- 60 F. Zhang, X. Liang, D. Li, X. Yin, X. Tian, B. Li, H. Xu, K. Guo and J. Li, *J. Mater. Chem. C*, 2019, **7**, 12328–12335.
- 61 H. Huang, Y. Zhou, Y. Wang, X. Cao, C. Han, G. Liu, Z. Xu, C. Zhan, H. Hu, Y. Peng, P. Yan and D. Cao, *J. Mater. Chem. A*, 2020, **8**, 22023–22031.
- 62 X. Yu, X. Li, Z. Cai, L. Sun, C. Wang, H. Rao, C. Wei, Z. Bian, Q. Jin and Z. Liu, *Chem. Commun.*, 2021, **57**, 5082–5085.
- 63 X. Feng, Y. Chen, Y. Lei, Y. Zhou, W. Gao, M. Liu, X. Huang and H. Wu, *Chem. Commun.*, 2020, **56**, 13638–13641.
- 64 Y. Qi, N. Ding, Z. Wang, L. Xu and Y. Fang, *ACS Appl. Mater. Interfaces*, 2019, **11**, 8676–8684.
- 65 W. Yuan, X. K. Ren, M. Li, H. Guo, Y. Han, M. Wu, Q. Wang, M. Li and Y. Chen, *Angew. Chem., Int. Ed.*, 2018, **57**, 6161–6165.
- 66 W. Yuan, J. Cheng, X. Li, M. Wu, Y. Han, C. Yan, G. Zou, K. Mullen and Y. Chen, *Angew. Chem., Int. Ed.*, 2020, **59**, 9940–9945.

